

PREPRINT — WORK IN PROGRESS

This document is a preprint: an early, incomplete version of a research paper shared publicly to establish priority, invite feedback, and make the concept available to the research community before peer review. It has not been peer reviewed. The system described is at the conceptual design stage — no prototype has been built yet. Numerical values for mass, force, cost, and performance are design estimates, clearly marked as such throughout. Sections marked [INCOMPLETE] are planned but not yet written. This document will be updated as the project develops.

Version 0.1 — April 2026 — Feedback welcome: xryh13@gmail.com

A BCI-Assisted Shape-Memory-Alloy Tentacle Arm

Conceptual Design and Feasibility Analysis for Industrial Worker Augmentation

Lloyd Axail Cordova Barrera

Independent Researcher

ORCID: 0009-0005-3424-9212

Abstract

Repetitive manual tasks in industrial production environments expose workers to sustained physical loads that elevate fatigue and the incidence of musculoskeletal disorders. Full automation addresses these risks but carries integration costs prohibitive for many small and medium manufacturers. This paper proposes a BCI-assisted tentacle-like mechanical arm actuated by shape memory alloy (SMA) wires as a worker augmentation device: a lightweight, modular soft-robotic limb controlled via non-invasive EEG-based motor imagery and supported by a compressed AI inference model running offline on a Raspberry Pi class embedded processor. The system is designed to extend the worker's effective physical capacity without replacing their decision-making role. This preprint presents the conceptual design — mechanical architecture, SMA actuation rationale, sensor suite, BCI paradigm selection, AI inference pipeline, implementation plan, evaluation methodology, and cost analysis — together with three conceptual design figures. A companion paper develops the embedded AI sub-system. The system has not yet been prototyped; all performance values are design estimates.

Keywords: *brain-computer interface; shape memory alloy; soft robotics; worker augmentation; motor imagery EEG; embedded AI; TinyML; industrial ergonomics; musculoskeletal disorders.*

1. Introduction

In many industrial production lines, repetitive manual tasks requiring visual inspection and fine motor control remain largely human-dependent. Activities such as inspecting LCD panels for defective pixels, sorting components by hand, or packaging goods involve continuous motion,

sustained static postures, and concentrated attention — conditions that elevate fatigue, error rates, and the incidence of musculoskeletal disorders (MSDs). Occupational health literature documents that work-related fatigue impairs reaction time and task performance, increasing the likelihood of both quality errors and workplace incidents [1], [2].

Full automation — industrial robot arms or specialized machines — addresses these problems but is not universally adopted. Designing, integrating, and maintaining task-specific automation requires custom vision systems, end-effectors, fixtures, and control logic, representing capital expenditures and integration costs that remain prohibitive for small and medium manufacturers or for low-volume, highly specialized tasks. The International Federation of Robotics reports that while average robot unit prices have declined, integration and deployment remain significant adoption barriers [3].

This paper proposes a BCI-assisted tentacle-like mechanical arm as a worker augmentation device: a modular soft-robotic limb, biologically inspired by cephalopod tentacle morphology, actuated by shape memory alloy wires, and controlled via non-invasive EEG-based motor imagery brain-computer interface. Rather than replacing the human operator, the system acts as an extension of the worker's body — an additional limb that does not fatigue — improving task consistency and reducing physical load while preserving full operator agency.

The system integrates four converging technological trends: (1) soft and continuum robotics enabling safe, adaptable manipulation in human-proximate workspaces [4]; (2) SMA actuators offering high force-to-weight ratio and silent operation without pneumatic infrastructure [5]; (3) non-invasive BCI achieving practical classification accuracy outside laboratory settings [6]; and (4) embedded AI enabling compressed neural networks to run locally without internet dependency [7].

Figure 1 provides a system-level overview of the proposed design. A companion paper develops the AI inference sub-system in detail.

Figure 1

System overview: vest-mounted BCI tentacle arm

The worker wears a back-mounted vest harness carrying the embedded processor (Raspberry Pi 4), battery, and motor drivers. Four SMA-actuated tentacle segments extend over the shoulder, terminating in a 3-finger soft gripper. The EEG headset transmits motor imagery signals to the processor via Bluetooth. The processor runs the distilled AI model offline, decodes motor commands, and drives the SMA wires via PWM current control. IMU, force, and temperature sensors in each segment provide closed-loop feedback. No internet connection is required during operation. [See companion interactive diagram — to be included in final version]

Figure 1. System overview: vest-mounted BCI-controlled SMA tentacle arm. The worker's own arms remain free. Electronics are carried on the vest; the arm extends over the shoulder.

2. Justification and Relevance

2.1 Occupational Health Benefits

Repetitive industrial tasks generate cumulative musculoskeletal load that manifests as work-related MSDs in the shoulder, neck, and upper extremities — the leading cause of occupational disability in manufacturing environments [1]. Passive and active assistive devices have demonstrated measurable load reductions: back exosuits have increased lifting endurance by 28–75% and reduced cumulative lumbar damage estimates by 27–93% [8]. Shoulder exoskeleton studies report reduced muscle activation and perceived effort during sustained overhead work [9]. These results establish that appropriately designed assistive devices can materially reduce MSD risk, motivating the augmentation approach proposed here.

The tentacle arm targets a different intervention point than exoskeletons: rather than supporting the worker's existing limbs, it provides an additional effector that takes on the load of the repetitive task, leaving the worker's arms available for higher-complexity or quality-checking functions. This division of labor is the primary ergonomic rationale for the tentacle form factor.

2.2 Productivity and Quality

Fatigue-related performance degradation in repetitive tasks is well documented: error rates increase and throughput decreases as shift duration extends [2]. A system that maintains consistent task execution without fatigue directly addresses both dimensions. The productivity argument does not require that the device operate faster than a human worker — only that it operate at a consistent rate throughout the shift without the degradation that human fatigue introduces.

2.3 Economic Rationale

For small and medium manufacturers whose production volumes do not justify bespoke fixed automation, a modular wearable assistive arm presents a plausible lower-cost alternative. Consumer-grade EEG headsets suitable for prototyping are available in the USD 200–800 range. SMA wire (Nitinol) is commercially available at approximately USD 5–50 per meter depending on diameter and supplier. Raspberry Pi class processors cost under USD 100.

A precise total cost estimate cannot be provided at this conceptual stage. The economic claim made here is bounded: this class of device is plausibly producible at lower unit cost than industrial passive exoskeletons (typically USD 1,000–5,000 per unit [9]) for production volumes above a few hundred units. This hypothesis will be evaluated quantitatively during the prototype phase.

2.4 Social and Equity Impact

Accessible assistive technology reduces the disparity between large manufacturers with capital for full automation and small firms without it. Reducing occupational MSD incidence lowers absenteeism, healthcare costs, and long-term disability. The offline-capable, internet-independent architecture also makes the system deployable in manufacturing environments without reliable connectivity.

3. State of the Art

3.1 Soft Robotics and Tentacle-Inspired Manipulators

Soft robotics has demonstrated effectiveness for handling fragile objects and operating in direct human contact. Bio-inspired designs — including octopus-inspired tentacle manipulators capable of continuous wrapping motions — achieve dexterity and compliance difficult to reproduce with rigid mechanisms [4], [10]. The E-SOAM integrates soft materials and embedded sensors for reaching and grasping with high flexibility [11]. Harvard's Soft Tentacle Robot and Festo's BionicSoftArm demonstrate tentacle form factor viability for adaptive grasping, though current designs face limitations in force output and dependence on pneumatic actuation requiring external air supply infrastructure [12], [13]. The present design addresses the pneumatic infrastructure limitation by substituting SMA wire actuation.

3.2 Shape Memory Alloy Actuators

Shape memory alloys — principally Nitinol (Ni-Ti) — change shape in response to thermal stimulus, contracting approximately 4% in length and generating large resistive force upon heating above the austenite transition temperature [5]. SMA displays one of the highest work densities among actuator materials at 10 J/cm^3 and can generate forces more than 100 times its own weight [5]. SMA wire actuated tendon systems have achieved bending angles up to 400° and tip forces of 0.89 N in soft gripper configurations [14].

The principal limitation of SMA actuators for repetitive industrial tasks is actuation frequency: cool-down by natural convection limits cycle rates to approximately 0.5–1 Hz for typical wire diameters used in soft robotic applications [15]. This is a significant constraint and must be addressed through wire diameter selection and task matching.

3.3 Industrial Exoskeletons

Industrial exoskeletons have demonstrated ergonomic benefits for reducing worker fatigue and MSD risk, with muscle load reductions reported above 30% when properly calibrated [8]. Adoption barriers include cost, lack of standardization, and comfort limitations during extended wear [9]. These limitations motivate lighter, more targeted augmentation devices rather than full-body exoskeletal systems.

3.4 Non-Invasive BCI and Motor Imagery EEG

Three EEG paradigms are relevant to this application: P300 event-related potentials (high accuracy, requires visual stimulus), SSVEP (high accuracy, requires visual stimulus), and motor imagery (lower accuracy, no external stimulus required). For a system used during visual inspection tasks, P300 and SSVEP are excluded because they require the worker to attend to an external visual stimulus, which conflicts with the visual attention the inspection task demands. Motor imagery is selected despite lower baseline classification accuracy because it is the only paradigm compatible with uninterrupted task performance [6].

3.5 Embedded AI for BCI

Knowledge distillation — training a compact student model to replicate a larger teacher model's behavior — has compressed EEG motor imagery classification models by up to 90% in size while maintaining competitive accuracy [21]. TinyML frameworks (TensorFlow Lite, ONNX Runtime) enable deployment of compressed neural networks on ARM Cortex-class processors at inference latencies below 100 ms [7]. The companion paper develops this sub-system fully.

3.6 Gap Identified

No published design integrates an SMA-actuated modular tentacle arm with motor imagery BCI control and an offline-capable embedded AI inference engine for industrial worker augmentation. The integration of SMA actuation with BCI control is particularly novel: SMA's silent operation, absence of pneumatic infrastructure requirements, and high force-to-weight ratio make it better suited than pneumatic actuation for a wearable industrial device, but its lower cycle frequency requires careful task-to-capability matching that has not been analyzed in the augmentation context.

4. Prototype Design

4.1 Biological Inspiration and Form Factor

The cephalopod tentacle provides the morphological template. Key properties: continuous compliance along the entire length enabling wrapping and contouring to irregular object surfaces; independent actuation of segments allowing complex trajectories from simple control inputs; and inherent mechanical safety because the limb yields under unexpected contact. These properties are well-suited to SMA wire actuation, which provides distributed contraction along embedded wires analogous to the longitudinal and transverse muscle fibers of the biological tentacle.

The proposed arm consists of four modular segments connected in series, each independently actuatable, mounted on a vest/back harness and extending over the shoulder. The modular design allows segment replacement, variable arm length, and potential future expansion to dual-arm configurations. The arm terminates in a soft gripping end-effector composed of three sub-segments arranged radially. Figure 2 shows the internal anatomy of a single segment.

Figure 2

Single segment: longitudinal and cross-sectional views

Left panel (longitudinal view): one 80–120 mm segment showing the outer silicone elastomer matrix (Ecoflex 00-30), three embedded SMA wires running the full segment length (shown as amber bars), a central structural spine channel (dashed), an IMU sensor at mid-segment, thermistors near each SMA wire bundle, and proximal/distal mechanical connectors at each end. A-A section line indicates the cross-section plane. Left bending arrow shows the direction of movement when SMA wire A contracts. Right panel (cross-sectional view, A-A): end-on view showing the three SMA wires (A, B, C) at 120° spacing within the silicone matrix, the central spine channel, the IMU at center, and thermistors adjacent to each wire. Activating wire A alone bends the segment toward A; activating B and C together bends it away from A. [Detailed engineering drawing to be added in v0.2]

Figure 2. Single tentacle segment in longitudinal section (left) and cross-section A–A (right). Three SMA wires at 120° spacing embedded in silicone matrix enable 3-axis bending. IMU and thermistors provide orientation and thermal feedback.

4.2 Actuation: SMA Wire Selection and Configuration

Nitinol SMA wire (Ni-Ti alloy, approximately 55% nickel by weight) is selected as the primary actuator. The wire is embedded in a silicone elastomer matrix in an antagonistic configuration: three wires arranged circumferentially actuate bending in three directions, and the passive elasticity of the matrix provides the restoring force when heating ceases.

Parameter	Design Estimate / Literature Basis
SMA wire diameter	150–250 μm (smaller = faster cooling, lower force per wire)
Actuation temperature	$\sim 70\text{--}90^\circ\text{C}$ (Nitinol austenite transition, standard)
Contraction ratio	$\sim 4\%$ of wire length (SMA literature standard)
Tip force per segment	0.5–1.5 N [ESTIMATE based on [14]]
Cycle frequency	0.5–1.0 Hz natural convection; 2–3 Hz with forced air [15]
Bending angle per segment	Up to 90° [ESTIMATE based on [14]]
Segment length	80–120 mm [ESTIMATE]
Segment mass	30–60 g including SMA, matrix, and sensors [ESTIMATE]

The 0.5–1.0 Hz natural convection cycle rate is the primary design constraint and must be matched to the task. LCD panel inspection and component sorting tasks typically involve hold-and-release cycles of 1–3 seconds per action, which is within the achievable range. Tasks requiring faster repetitive motion are outside the scope of this design without active cooling.

4.3 Structural Materials and Mechanical Architecture

The arm matrix is silicone elastomer (Shore A hardness 20–40). The attachment harness uses a lightweight carbon fiber composite frame padded with EVA foam, distributing load across the shoulder and upper back.

- **Degrees of freedom (DOF):** 3 per segment (bending in three planes); 4 segments = 12 total DOF [ESTIMATE].
- **Total arm length:** 320–480 mm extended [ESTIMATE].
- **Total system mass (arm + harness + electronics):** 600–900 g [ESTIMATE].
- **Payload target:** 200–500 g at the tip [ESTIMATE].

4.4 Sensor Suite

- **IMUs (one per segment):** 6-DOF (accelerometer + gyroscope) for segment orientation tracking. Target: MPU-6050, mass < 1 g, power < 5 mW.
- **Force sensors at end-effector:** thin-film FSRs at each gripper sub-segment for grasp detection and slip prevention.
- **Temperature sensors on SMA wires:** embedded thermistors per actuated wire bundle for closed-loop thermal control, preventing overheating beyond 120°C .

- **EEG headset:** consumer-grade dry-electrode EEG, 8–16 channels, 250–500 Hz sampling.

4.5 Ergonomics and Attachment Interface

The arm attaches via a shoulder-mounted harness. Design requirements: distribute arm mass across shoulder and upper back; permit rapid donning and doffing without tools; accommodate a range of body sizes; allow unrestricted movement of the worker's own arms. These requirements are drawn from the wearable robotics usability literature, which identifies donning burden and range-of-motion restriction as primary adoption barriers [9].

[ESTIMATE — to be validated in prototype phase] Total harness + arm mass presented to the worker's body: 600–900 g, distributed across shoulder and upper back.

5. Control and Movement

Figure 3 shows the complete signal and control flow from EEG acquisition through to SMA actuation.

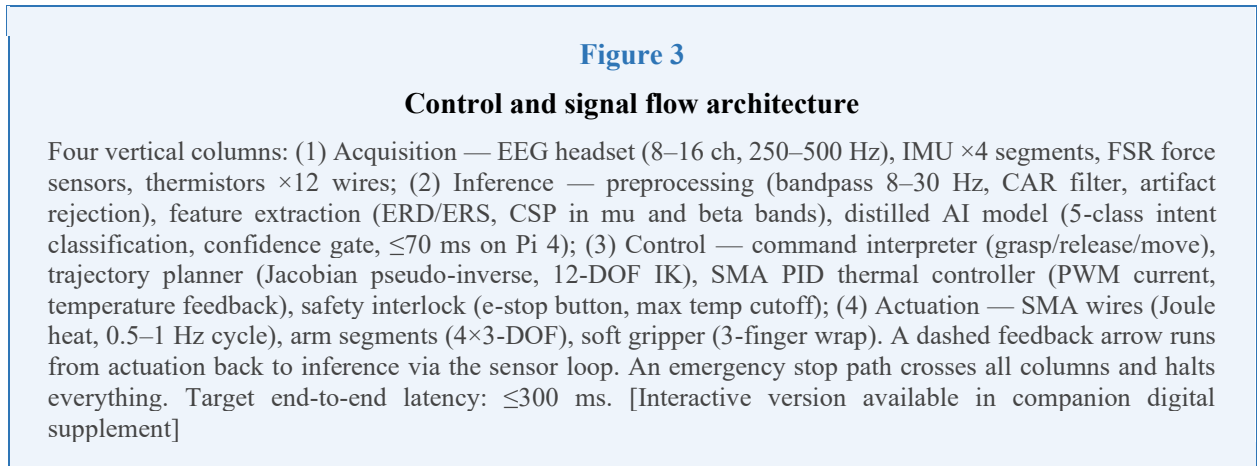


Figure 3. Signal and control flow from EEG acquisition to SMA actuation. Dashed arrows indicate feedback paths. The confidence gate prevents low-confidence EEG classifications from triggering arm motion. Emergency stop overrides all columns simultaneously.

5.1 BCI Paradigm and Signal Acquisition

Motor imagery BCI is selected as the control paradigm. The worker imagines performing a specific movement generating classifiable EEG patterns in the sensorimotor cortex without executing the physical movement. This paradigm is selected over P300 and SSVEP because it does not require attention to an external visual stimulus, preserving the worker's visual focus for the inspection or manipulation task.

EEG is acquired at 250–500 Hz, bandpass-filtered to 8–30 Hz (μ and β bands), and processed in windows of 250–500 ms with 50% overlap.

5.2 Signal Processing Pipeline

- **Preprocessing:** bandpass filter (8–30 Hz), common average reference (CAR), artifact rejection (amplitude threshold and kurtosis-based).
- **Feature extraction:** event-related desynchronization/synchronization (ERD/ERS) in μ (8–12 Hz) and β (13–30 Hz) bands; common spatial patterns (CSP).
- **Classification:** distilled embedded model classifies into five command classes: grasp, release, move proximal, move distal, hold. Below-threshold confidence produces a hold command.

5.3 Motion Control

- **Trajectory planning:** inverse kinematics using Jacobian pseudo-inverse, appropriate for low-speed operation of the target task class.
- **SMA thermal control:** PID controller on wire temperature, setpoint determined by desired contraction level, feedback from embedded thermistors.
- **Safety interlock:** physical emergency stop accessible to the worker's free hand at all times. Arm returns to rest position and deactivates SMA heating on stop signal.

6. Artificial Intelligence and Local Predictive Model

6.1 Role of the AI Module

The AI module performs two functions: motor intention prediction (anticipating the user's next command before an explicit classification threshold is reached, reducing effective control latency) and trajectory smoothing (converting discrete command outputs into continuous motion trajectories, avoiding abrupt motion).

6.2 Model Architecture and Compression

A large teacher model — a multi-layer Transformer trained on public EEG motor imagery datasets (BCI Competition IV 2a, 2b) plus session-specific calibration data — is trained offline. A compact student model is trained via knowledge distillation, reducing model size by approximately 80–90% while retaining competitive classification accuracy [21]. The student model is then quantized to 8-bit integer precision using TensorFlow Lite and deployed to the Raspberry Pi embedded processor.

[ESTIMATE — to be validated in prototype phase] Inference latency for the student model on Raspberry Pi 4: 30–70 ms per 500 ms EEG window. End-to-end latency: 150–300 ms. Target: below 300 ms.

6.3 Per-Subject Calibration

Before each work session, the worker performs a calibration protocol of approximately 5–10 minutes (20–40 imagined movement trials per class). Session-specific data is used to fine-tune only the final classification layer of the student model on-device — computationally feasible on the embedded processor.

6.4 Offline Operation and Data Privacy

The model runs entirely on the embedded processor. No EEG data is transmitted externally at any point. Calibration data is stored locally in encrypted form. This architecture addresses neural data privacy requirements structurally rather than through policy alone.

Full specification of the model architecture, training pipeline, and compression methodology is provided in the companion paper.

7. Ethical, Social, and Labor Implications

7.1 Worker Health, Autonomy, and Dependency

The system is designed to enhance human performance, not replace it. The design requires instant manual override, emergency shutdown without BCI input, and adjustable assistance levels. Preventing functional dependency requires that the device be designed for easy removal and that workers be evaluated on their unassisted capability during regular periods.

7.2 Neural Data Privacy and Security

EEG signals are sensitive biometric data. The offline embedded architecture addresses this structurally: signals are never transmitted externally. Workers must provide informed consent before calibration and must be able to withdraw consent and request deletion of their calibration data at any time.

7.3 Equity, Training, and Access

The design must prioritize ease of calibration, intuitive operation, and maintainability by non-specialist workers. Training programs for calibration, safe operation, and routine maintenance are a necessary component of responsible deployment, not an afterthought.

7.4 Regulatory Compliance and Responsibility

The system targets compliance with ISO 13482:2014 (safety requirements for personal care and assistive robots) and the EU Machinery Directive 2006/42/EC [22], [23]. A shared-responsibility framework is proposed: the manufacturer guarantees system safety within specified operating conditions; the operator retains decision-making control for use within those conditions.

7.5 Labor Displacement

The worker augmentation framing is a genuine design commitment. However, the possibility that augmented workers displace non-augmented workers, or that productivity gains enable headcount

reduction, must be acknowledged as a deployment risk. These outcomes depend on employer decisions, not on the technology itself.

8. Practical Implementation

8.1 Hardware Stack

Component	Specification / Candidate
Embedded processor	Raspberry Pi 4 Model B (ARM Cortex-A72, 1.8 GHz, 4 GB RAM)
EEG headset	OpenBCI Cyton (8-channel, 250 Hz) or Emotiv EPOC+ (14-channel)
IMU per segment	MPU-6050 (6-DOF, I ² C, 3.3V, < 1 g)
Force sensors	Interlink FSR 400 or equivalent thin-film FSR
Temperature sensors	NTC thermistor 10k Ω or IR thermopile (MLX90614)
SMA wire	Nitinol 150–250 μ m diameter, Dynalloy Flexinol or equivalent
Elastomer matrix	Smooth-On Ecoflex 00-30 or Dragon Skin 10
Motor drivers / PWM	L298N H-bridge or MOSFET array for SMA current control
Power supply	LiPo 11.1V 3S pack, minimum 3000 mAh [ESTIMATE]
Harness frame	Carbon fiber composite + EVA foam padding
Communication	Bluetooth 5.0 (EEG to Pi); I ² C bus (IMU/sensors to Pi)

8.2 Software Stack

- **OS:** Raspberry Pi OS Lite (headless).
- **AI inference:** TensorFlow Lite runtime.
- **EEG acquisition:** Brainflow library (headset-agnostic).
- **Signal processing:** NumPy, SciPy (bandpass filtering, CSP, feature extraction).
- **Control loop:** Python with real-time scheduling; 20–50 Hz for IMU feedback; 2–4 Hz for BCI command update.
- **Logging:** SQLite local database, encrypted at rest.

8.3 Development Timeline

Phase	Activities and Duration
-------	-------------------------

Phase 1: Component validation (Months 1–4)	Fabricate and test single SMA-actuated segment. Benchmark EEG classification on embedded processor using BCI Competition IV public dataset. Validate inference latency and power draw.
Phase 2: Integration and bench test (Months 5–8)	Integrate 3-segment arm, sensor suite, and processor. Measure end-to-end latency. Evaluate calibration protocol with $N \geq 5$ subjects. EMG measurement of worker load with and without device.
Phase 3: Task evaluation (Months 9–12)	Full 4-segment arm. Two representative industrial task scenarios. $N \geq 10$ subjects. Task completion rate, error rate, throughput, NASA-TLX, SUS. Safety incident documentation.
Phase 4: Iteration and cost analysis (Months 13–16)	Design refinement based on Phase 3 findings. Full bill of materials cost analysis. Manufacturing process evaluation for small-batch production.

9. Evaluation and Performance Metrics

9.1 Technical Metrics

Metric	Target / Measurement Method
End-to-end latency (EEG to arm motion)	< 300 ms; synchronized timestamp logging
Motor imagery classification accuracy	$\geq 80\%$ per-subject after calibration; 5-fold cross-validation
SMA actuator cycle rate	≥ 0.5 Hz sustained; infrared thermometry + motion capture
Tip force	≥ 200 g payload; calibrated force gauge at end-effector
Segment bending range	$\geq 60^\circ$ per bending direction; motion capture
Total system mass	≤ 1 kg; laboratory scale
Inference latency on Pi 4	< 100 ms; profiled with TFLite benchmark tool

9.2 Ergonomic and Usability Metrics

- **Muscle load:** surface EMG on trapezius, deltoid, and forearm flexors during simulated tasks. Target: no increase in EMG amplitude relative to unassisted baseline.
- **Subjective workload:** NASA-TLX questionnaire after each task scenario.
- **Usability:** System Usability Scale (SUS). Target: $SUS \geq 68$.
- **Calibration time:** Target: ≤ 10 minutes from headset donning to system ready.

9.3 Comparative Evaluation

Task completion rate, error rate, and throughput are measured in three conditions: (A) unassisted worker, (B) worker with device, (C) simulated fixed automation baseline. The device does not

need to match Condition C — it needs to improve on Condition A while remaining below the cost of implementing Condition C.

10. Cost Analysis and Economic Viability

10.1 Prototype Bill of Materials

Component	Estimated Unit Cost (USD)
Raspberry Pi 4 (4 GB)	55–75
EEG headset (OpenBCI Cyton)	450–500
IMU sensors × 4	4–12 total
FSR sensors × 6	10–20 total
Thermistors × 12	4–8 total
Nitinol SMA wire (4 m)	20–60
Silicone elastomer (Ecoflex 00-30, 1 kg)	30–50
Motor drivers / MOSFET array	10–20
LiPo battery pack	20–40
Carbon fiber harness frame (custom)	80–150
Miscellaneous (connectors, PCB, enclosure)	50–100
TOTAL PROTOTYPE ESTIMATE	733–1,035 USD [ESTIMATE]

These are component-level estimates for a single hand-assembled prototype. They do not include engineering time, tooling, testing equipment, or certification costs.

10.2 Comparison with Alternatives

Solution	Approximate Cost	Notes
Fixed automation (custom)	USD 50,000–500,000+	Per task; high integration cost
Collaborative robot arm	USD 25,000–60,000	General purpose; requires programming
Industrial passive exoskeleton	USD 1,000–5,000	No active control; no AI
Advanced BCI prosthetic (clinical)	USD 10,000–100,000+	Medical grade; often invasive

Proposed system (production target)	USD 800–1,500 [ESTIMATE]	Wearable; BCI; offline AI
-------------------------------------	--------------------------	---------------------------

10.3 Operating Costs

SMA wire fatigue life: typically 100,000–1,000,000 cycles depending on strain amplitude and cooling conditions [15]. At 0.5 Hz for 6 hours per day \approx 10,800 cycles per day. Conservative wire replacement interval: every 3–10 months per segment [ESTIMATE]. Wire cost per replacement: under USD 5 per segment. Total system power: approximately 8–18 W [ESTIMATE], providing 4–8 hours operation per battery charge.

11. Limitations, Challenges, and Future Improvements

11.1 Current Technical Limitations

- **SMA cycle frequency:** the 0.5–1.0 Hz natural convection limit restricts the system to tasks with action cycles of 1 second or longer. Tasks requiring faster motion are outside the current design envelope without active cooling.
- **Motor imagery classification accuracy:** baseline accuracy of 70–85% in realistic conditions means approximately 1 in 7 to 1 in 5 commands may be misclassified. The confidence-threshold gating strategy mitigates this but does not eliminate it.
- **Inter-session EEG signal drift:** EEG features drift between sessions and across the workday, requiring per-session calibration.
- **SMA hysteresis and nonlinearity:** SMA actuation exhibits significant hysteresis between heating and cooling phases. Precise position control requires model-based or adaptive compensation.
- **Payload capacity:** the estimated 200–500 g tip payload is adequate for the target task class but insufficient for heavier industrial manipulation.

11.2 Potential Future Improvements

- **Hybrid SMA + cable actuation:** combining SMA for low-speed tasks with cable-driven actuation for higher-speed positioning could extend the operational envelope.
- **Active cooling:** a thermoelectric cooler per segment would increase cycle rate to 3–5 Hz at the cost of added mass and power draw.
- **Continuous on-device learning:** allowing the model to update from post-session feedback without transmitting data externally would improve long-term cross-session performance.
- **Multi-arm configuration:** dual-arm attachment with bilateral BCI control would double effective manipulation capability.
- **Materials:** lower-density silicone formulations and carbon fiber composite housings could reduce total arm mass below 400 g.

12. Work in Progress: Sections Not Yet Complete

Section	Status / What is planned
Engineering drawings	CAD models and detailed mechanical drawings for each segment, harness, and connector. To be added in v0.2 once segment geometry is finalized.
Kinematics and workspace envelope	Formal kinematic analysis of the 12-DOF arm. Reachable workspace diagram. Jacobian derivation. Planned for v0.3.
Prototype photos / results	No prototype built yet. Photos, force measurements, and latency test results will be added as the prototype is developed (Phase 1 target: Month 4).
AI companion paper	Separate paper developing the distilled motor intention prediction model architecture, training pipeline, compression methodology, and embedded benchmarks. In preparation.
User study data	No subjects tested yet. Phase 2 and 3 of the validation plan (Sections 8.3 and 9) will produce this data. Target: Month 8 onward.

Readers and potential collaborators are invited to contact the author with feedback, critique, or interest in contributing to the prototype development phase. This preprint will be updated as each section is completed.

13. Conclusion

This preprint has presented the conceptual design and feasibility analysis for a BCI-assisted SMA tentacle arm for industrial worker augmentation. The proposed system addresses a real and documented problem — MSD risk and fatigue in repetitive industrial tasks, and the cost barrier to full automation for small and medium manufacturers — by integrating soft robotic manipulation, SMA actuation, non-invasive EEG motor imagery BCI, and offline embedded AI inference into a single wearable platform.

The selection of SMA wire actuation over pneumatic or cable-driven alternatives is motivated by the absence of external infrastructure requirements, silent operation, and high force-to-weight ratio. The primary trade-off — limited cycle frequency due to thermal cool-down — is stated explicitly and addressed through task matching. All numerical estimates are clearly marked as design targets pending prototype validation.

Three conceptual design figures have been presented: a system overview (Figure 1), a single-segment cross-section showing the internal SMA and sensor arrangement (Figure 2), and the complete control and signal flow architecture (Figure 3). These figures, together with the design rationale and feasibility analysis, constitute the current contribution of this preprint.

The immediate next steps are: (1) fabricate and test a single SMA-actuated segment to validate the actuation estimates; (2) benchmark the distilled EEG classification model on the target embedded

hardware; and (3) publish the companion paper developing the AI inference sub-system. Updates will be issued as each milestone is reached.

References

- [1] C. O. Soares et al., "Preventive Factors Against Work-Related Musculoskeletal Disorders: A Systematic Review," *BMC Musculoskeletal Disorders*, vol. 21, 2020.
- [2] National Institute for Occupational Safety and Health (NIOSH), *Musculoskeletal Disorders and Workplace Factors*, U.S. Dept. of Health and Human Services, Publication No. 97-141, 1997.
- [3] International Federation of Robotics (IFR), *World Robotics: Industrial Robots 2022 — Executive Summary*, 2022.
- [4] O. Yasa, "An Overview of Soft Robotics," *Annual Review of Control, Robotics, and Autonomous Systems*, vol. 6, pp. 111–133, 2023.
- [5] A. Sayed et al., "Control Aspects of Shape Memory Alloys in Robotics Applications: A Review over the Last Decade," *Actuators (MDPI)*, 2022.
- [6] O. Maslova et al., "Non-invasive EEG-based BCI Systems from the Beginning to Now," *Frontiers in Human Neuroscience*, vol. 17, 2023.
- [7] Y. Abadade et al., "A Review on the Emerging Technology of TinyML," *ACM Computing Surveys*, 2023.
- [8] L. Ralfs et al., "Insights into Evaluating and Using Industrial Exoskeletons," *Ergonomics*, vol. 66, no. 9, pp. 1221–1235, 2023.
- [9] T. Ma, "Modeling for Design and Evaluation of Industrial Exoskeletons: A Systematic Review," *IEEE Transactions on Human-Machine Systems*, vol. 53, no. 2, 2023.
- [10] W. Li, "Actuation Mechanisms and Applications for Soft Robots," *Applied Sciences*, vol. 13, no. 16, 2023.
- [11] Z. Xie et al., "Octopus-Inspired Sensorized Soft Arm for Environmental Interaction," *Science Robotics*, vol. 8, no. 73, 2023.
- [12] Harvard SEAS, "Soft Tentacle Robot Capable of Grasping Fragile Objects," *Harvard School of Engineering and Applied Sciences*, 2020.
- [13] Festo AG, "BionicSoftArm: Modular Soft Robotic Arm for Human Collaboration," *Festo Technical Report*, 2022.
- [14] T. George Thuruthel et al., "Long Shape Memory Alloy Tendon-based Soft Robotic Actuators and Implementation as a Soft Gripper," *Scientific Reports*, 2019.
- [15] A. Villoslada et al., "Characterization and Analysis of a Flexural Shape Memory Alloy Actuator," *Actuators*, vol. 10, no. 8, 2021.
- [16] Q. Y. Hamid et al., "Shape Memory Alloys Actuated Upper Limb Devices: A Review," *Sensors and Actuators Reports*, vol. 5, 2023.
- [17] D. Shin et al., "Woven Fabric Muscle for Soft Wearable Robotic Application Using Two-Dimensional Zigzag SMA Actuator," *Soft Robotics*, 2024.

- [18] E. Shi et al., "Adaptive Control for Shape Memory Alloy Actuated Systems with Applications to Human-Robot Interaction," *Frontiers in Neuroscience*, vol. 18, 2024.
- [19] Y. Liu et al., "CTNet: A Convolutional Transformer Network for EEG-Based Motor Imagery Classification," *Scientific Reports*, 2024.
- [20] A. Craik et al., "Design and Validation of a Low-Cost Mobile EEG-Based Dry-Electrode Headset," *Frontiers in Neuroscience*, vol. 17, 2023.
- [21] W. Zhang et al., "A Multi-level Teacher Assistant-based Knowledge Distillation Framework for Motor Imagery EEG Decoding," *Neural Networks*, 2025.
- [22] ISO, ISO 13482:2014 — Robots and Robotic Devices: Safety Requirements for Personal Care Robots, 2014.
- [23] European Union, Directive 2006/42/EC on Machinery, *Official Journal of the EU*, 2006.